Science and Technology Infusion Climate Bulletin
NOAA's National Weather Service
43rd NOAA Annual Climate Diagnostics and Prediction Workshop
Santa Barbara, CA, 23-25 October 2018

Santa Ana Events in California: Global Scale Teleconnections and Potential Subseasonal to Seasonal Predictability

Tom Murphree[1], Emily Szasz[1, 2], and LT Kellen Jones, USN[1]
[1]*Department of Meteorology, Naval Postgraduate School, Monterey, CA*
[2]*University of Southern California*

1. Introduction

Wildfires in California have been especially destructive in recent years (*e.g.*, Keeley et al. 2009; Guzman-Morales et al. 2016; Mass and Owens 2019). Many of the most destructive fires have occurred in association with strong low-level, offshore, downslope synoptic wind events that occur during or soon after the end of the dry season (September-December). In southern California, especially coastal southern California, these offshore wind events are commonly referred to as Santa Ana events (*e.g.*, Raphael 2003; Rolinski *et al.* 2019). In other parts of California and western North America, dynamically similar offshore downslope wind events may be given different names (*e.g.*, Diablo winds in and near the San Francisco region; *cf.* Blier 1998). These wind events are forced by pressure gradient forces directed away from a low-level region of high pressure over or near the Great Basin and are most common in October-March (*e.g.*, Raphael 2003; Rolinski *et al.* 2019).

Santa Ana (SA) events typically last one to five days, but can last ten days or more (*e.g.*, Raphael 2003; Rolinski *et al.* 2019). SA winds increase the risk of serious wildfires, especially if they occur during or soon after the end of the summer dry season in the western US. The wildfires can, in turn lead to major societal disruptions (*e.g.*, loss or lives and property, evacuations, closings of schools and businesses, electric power outages; *e.g.*, Westerling *et al.* 2004; Keeley *et al.* 2009; Mass and Owens 2019).

We have conducted a preliminary investigation of how SA events are related to global scale, subseasonal to seasonal (S2S) processes. Our initial focus has been on characterizing and analyzing the global scale S2S anomalies associated with the development of SA events, as opposed to the synoptic to mesoscale focus of many prior studies of SA events (*e.g.*, Raphael 2003; Mass and Owens 2019). Our initial results indicate that: (a) global scale S2S processes are important in initiating SA events; and (b) variables associated with these processes may be useful predictors of SA favorable conditions at S2S lead times. The ability to skillfully predict these conditions could potentially improve the preparation for, and responses to, SA events. Jones *et al.* (2010) and Rolinski *et al.* (2019) discussed approaches to forecasting of SA events, but found low skill at S2S lead times (greater than about a week).

Our primary research questions were:

1. How are SA conditions over southern California (and dynamically related events over western North America) related to global scale climate variations?
2. What processes set up these conditions over southern California and western North America?
3. Can climate variation information be used to improve the understanding and prediction of these events?
4. What is the potential for skillful S2S prediction of these events?
5. What can we learn from these events about related S2S variations in western North America (*e.g.*, dynamically related temperature and precipitation anomalies in Alaska and the Great Plains)?

2. Data and methods

Our study region was global, especially the global tropics and extratropical northern hemisphere, but with a focus on western North America and especially southern California. Our study period was October-March 1974-2019, with a focus on November 1974-2018. We chose November as a focus month because: (a) November occurs after the dry season and, typically, before the start of substantial wet season precipitation in

Correspondence to: Tom Murphree, Department of Meteorology, Naval Postgraduate School, Monterey, CA;
E-mail: murphree@nps.edu

the western US; and (b) a number of major wildfires associated with SA events have occurred in November (*e.g.*, the Camp Fire and Woolsey Fire in November 2018; *e.g.*, Cappucci 2018).

Our main variables and data sets were:

1. Daily and monthly mean atmospheric circulation variables and SST from the R1 and CFSR reanalysis data sets (Kalnay *et al.* 1996; Saha *et al.* 2010)
2. Bimonthly El Niño, La Nina, and neutral (non-El Niño and non-La Niña) information from the Multivariate El Niño Index (MEI) data set interpolated to monthly means (Wolter and Timlin 2011)
3. Daily mean Madden-Julian Oscillation (MJO) information obtained from the Bureau of Meteorology (Wheeler and Hendon 2004)

From the R1 and CFSR data, we created an index of SA events based on the area-averaged 850 hPa zonal wind (u850) over coastal southern California. This region extends from Santa Barbara to San Diego and includes both ocean and land. We used u850 for our SA index based on prior studies that indicate that the zonal wind is a good indicator of the occurrence of SA conditions (*e.g.*, Guzman-Morales 2016), and because the winds at 850 hPa facilitate the identification of periods of offshore flow in both low lying terrain (*e.g.*, over the ocean) and elevated terrain (*e.g.*, the coastal mountains of southern California). We identified SA events as periods in which the area-averaged, three-day running mean value of u850 in the southern California region was negative. The dates, numbers, and durations of the SA events that we identified using this method are very similar to those found in other studies using different methods for identifying SA events (*e.g.*, Raphael 2003; Jones *et al.* 2010; Guzman-Morales 2016).

We analyzed the anomalies for several variables for the SA dates that we identified, and 45 days before and after those dates. Our focus was on tropical and extratropical anomalous 850 and 200 hPa geopotential heights (ZA850 and ZA200) and tropical outgoing longwave radiation (OLRA). In particular, we analyzed the five-day mean anomalies for: (a) individual SA events in November 1974-2018; and (b) composites of multiple SA events in November 1974-2018. The composites represented different numbers of events, depending on the conditions we applied in the selection of the events. These conditions represented, for example the: (a) intensity and duration of the SA events; and (b) occurrence, phase, and intensity of climate variations (*e.g.*, El Niño-La Niña, MJO).

We used the resulting anomaly patterns to identify: (a) the temporal evolution of global scale anomalies associated with SA events; (b) teleconnections associated with SA events; and (c) precursors and potential predictors of SA events.

In this article, we focus on our results for SA events occurring in November. But these results are representative of our results for SA events in other months and for dynamically similar events in other parts of western North America.

3. Results

Figure 1 shows ZA850 for a major SA event in late October 2003 that contributed to several very destructive wildfires in southern California (*e.g.*, Westerling *et al.* 2004). The schematic black arrows in Figure 1 represent the corresponding wind anomalies. The positive ZA850 over western North America and offshore wind anomalies over southern California and much of the western US are typical of SA events, as are onshore wind anomalies over coastal British Columbia and southern Alaska.

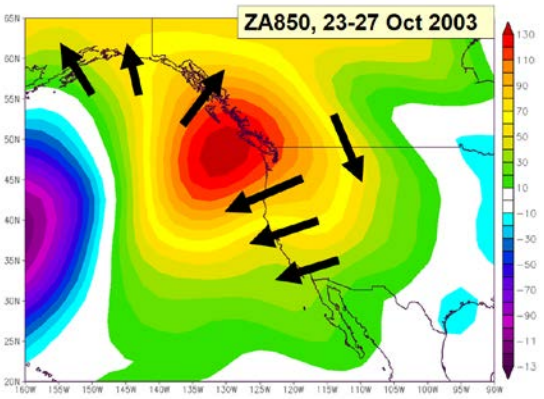

Fig. 1 Geopotential height anomalies at 850 hPa (ZA850) for 23-27 October 2003, a period in which during a major Santa Ana event and multiple wildfires occurred in southern California. The black arrows schematically indicate the associated wind anomalies at 850 hPa.

Figure 2 shows ZA200 for the late October 2003 SA event, and for two other SA events in mid-November 2008 and early December 2017 that were also associated with major wildfires in southern California (*e.g.*, Keeley *et al.* 2009; Guzman-

Morales 2016). Figure 3 shows ZA200 for a composite of the upper tercile of November SA events during the study period based on the magnitude of the u850 winds in coastal southern California (*i.e.*, the tercile with most offshore u850 winds). In all of the cases shown in Figures 2-3, there is: (a) a positive anomaly over western North America centered between 45-55 north latitude; and (b) an approximately zonal pattern of alternating positive and negative anomalies extending around the northern hemisphere extratropics (at about 20-70 north latitude). This zonal pattern of alternating positive and negative anomalies shown in Figures 2-3 indicates an anomalous planetary wave train with a zonal wave number 4-5 structure, with the strongest anomalies in the East Asia - North Pacific - North America region.

Figure 4 shows ZA200 for all days of the six Novembers with the greatest SA activity (the largest number of SA days), which were November 1976, 1980, 1989, 1992, and 2007. Note that the anomaly patterns are similar to those in Figures 2-3, although the anomalies are less pronounced over South Asia and there is more arcing in the wave train over the North Pacific and North America.

Animations of the ZA200 anomalies 45 days before and after individual and composite SA events in southern California (not shown) reveal that the anomalous wave trains shown in Figures 2-4 tend to: (a) develop as quasi-stationary wave trains that are first evident over South and East Asia two to four weeks prior to the SA events; and (b) then become more evident successively further to the east via eastward energy propagation into the North Pacific, North America, and North Atlantic.

These results indicate that SA events tend to be part of a global scale pattern of S2S anomalies that originates in the South Asia - East Asia sector several weeks prior to the SA events. These anomalies suggest that SA events are generated, at least in part, by anomalous wave train activity that teleconnects Asia to western North America. The MJO, and associated wave trains and teleconnections, have been identified as important factors in generating other types of anomalous conditions in western North America (*e.g.*, temperature and precipitation anomalies), with the western North American anomalies lagging the initiating MJO conditions by two or more weeks (*e.g.*, Higgins et al. 2000; Mundhenk *et al.* 2018).

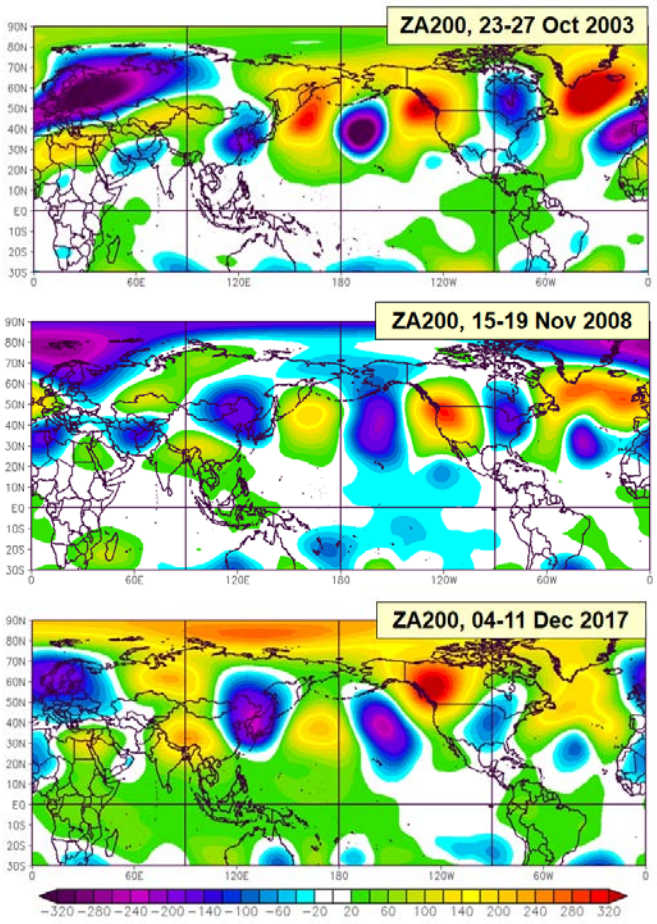

Fig. 2 Geopotential height anomalies at 200 hPa (ZA200) for 23-27 October 2003, 15-19 November 2008, and 04-11 December 2017. In each period, a major Santa Ana event and multiple wildfires occurred in southern California.

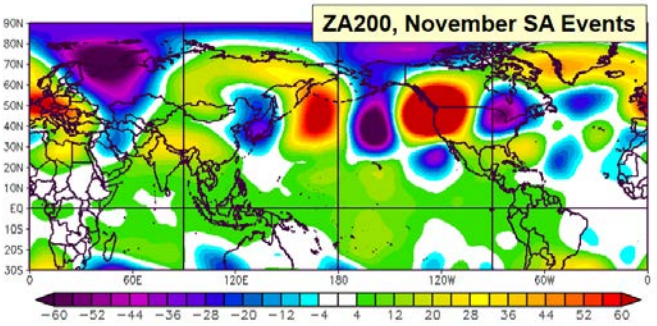

Fig. 3 Geopotential height anomalies at 200 hPa (ZA200) composited for the strongest Santa Ana events in southern California in November (the uppermost tercile of Santa Ana events).

This led us to investigate the MJO activity occurring several weeks prior to SA events. Figure 5 shows the November composite ZA200 for 20 days after MJO phase 2. In this phase, the convective component of the

MJO occurs in the central tropical Indian Ocean and the convective component occurs in the tropical western Pacific (*e.g.*, Madden and Julian 1994). Note in Figure 5 the zonally oriented anomalous wave train with zonal wave number 4-5 structure in the northern midlatitudes, with a positive anomaly over western North America, similar to the composite ZA200 patterns based on SA events (see Figures 2-4 and the corresponding text).

Animations (not shown) of ZA200 based on phase 2 based composites (such as the composite in Figure 5) reveal an evolution of the extratropical anomalous wave train that is similar to that for the ZA200 composite based on SA events (such as that shown in Figure 3). These results indicate that MJO phase 2 may be an important factor in initiating SA events. Other results (not shown) indicate that phases 8, 1, and 3 (phases with anomalies that are similar to phase 2) may also contribute to the initiation of SA events.

Prior studies (*e.g.*, Raphael and Finley 2007; Guzman-Morales 2016; Rolinksi *et al.* 2019) have investigated the associations between El Niño, La Niña, and SA events. We found that El Niño and La Niña can alter the global scale anomaly patterns associated with SA events and with MJO phases 8-1-2-3. As an example, Figure 6a (6b) shows the November composite ZA200 for 20 days after MJO phase 2, similar to Figure 5, but with only neutral and El Niño (La Niña) days included in the composite. That is, La Niña (El Niño) days were excluded from the compositing for Figure 6a (6b). A comparison of Figures 5 and 6 indicates that El Niño and La Niña events can alter how MJO sets up SA conditions over western North America. In particular, these events can alter the overall extratropical anomalous wave train associated with MJO phase 2, including the location and orientation of the positive anomaly over western North America and, thereby alter the corresponding wind anomalies over southern California.

4. Conclusions

Our results indicate that SA favorable conditions in southern California (and related events elsewhere in the western US) are part of anomalous global S2S processes. The MJO, especially phase 1, 2, and 3, appears to be important in initiating these processes at lead times of several weeks. El Niño and La Niña may be important in modifying how MJO initiates SA favorable

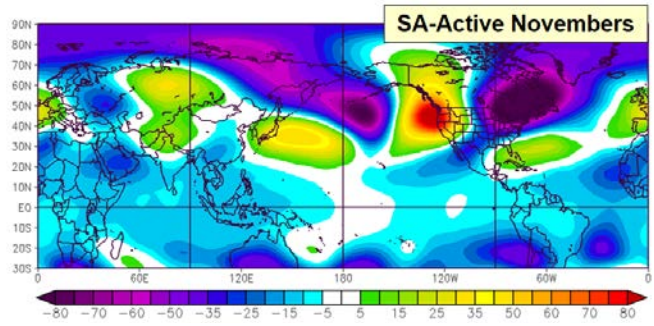

Fig. 4. Geopotential height anomalies at 200 hPa (ZA200) composited for the six Novembers with the most Santa Ana activity in southern California.

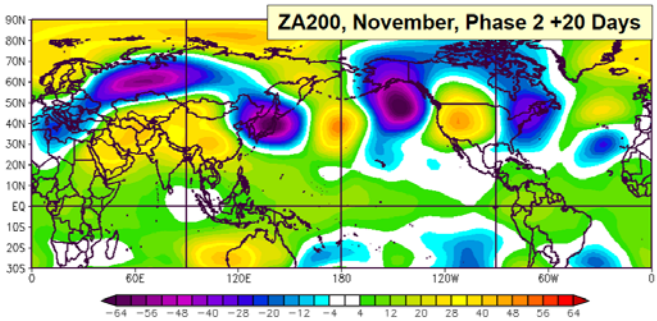

Fig. 5. Geopotential height anomalies at 200 hPa (ZA200) composited for all November days occurring 20 days after MJO phase 2.

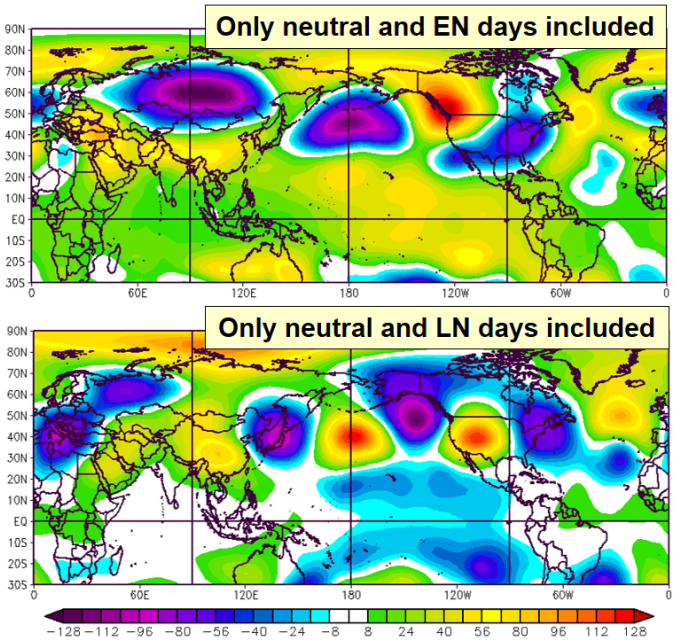

Fig. 6. Geopotential height anomalies at 200 hPa (ZA200) composited for November days occurring 20 days after MJO phase 2 but with: (a) only neutral and El Nino days included (upper panel); (b) only neutral and La Nina days included (lower panel).

conditions. The lead times associated with the process that create SA favorable conditions suggest that skillful S2S forecasting of these conditions may be possible. However, such forecasting would likely be complicated by the multiple processes that affect the setup of the extratropical anomalies associated with SA favorable conditions (*e.g.*, other climate variations, such as the Indian Ocean Dipole and the Arctic Oscillation; the extratropical background flow and other extratropical dynamic factors that help determine the wave train response to climate variations; *e.g.*, Sardeshmukh and Hoskins 1988).

The global scale pattern of anomalies that are favorable for SA conditions in southern California are also favorable for substantial anomalies in other variables and/or other locations. These include, for example, offshore wind anomalies over much of California and Oregon, and onshore wind anomalies and positive low-level temperature anomalies over southern Alaska. More generally, our initial results show that SA favorable anomalies tend to be part of a pattern of anomalous tropospheric ridging occurring over much of western North America. These larger scale anomalies support a wide range of anomalies that tend to extend from Alaska to northern Mexico and from the eastern North Pacific to central North America (*cf.* Swain *et al.* 2017). These preliminary findings suggest that improved understanding of the processes that generate anomalous ridging over western North America may contribute to a better understanding and prediction of SA events plus a wide range of related anomalies.

References

Blier, W., 1998: The Sundowner winds of Santa Barbara, California. *Wea. Forecasting*, **13**, 702–716, doi:10.1175/1520-0434(1998)013,0702:TSWOSB.2.0.CO;2.

Cappucci, M, 2018: After the fire disaster in Paradise, meteorologists mull how to improve warning system. *The Washington Post*, https://www.washingtonpost.com/weather/2018/11/28/after-fire-disaster-paradise-meteorologists-mull-how-improve-warning-system/?utm_term=.7b0f2c813

Guzman-Morales, J., A. Gershunov, J. Theiss, H. Li, and D. Cayan, 2016: Santa Ana winds of Southern California: Their climatology, extremes, and behavior spanning six and a half decades, *Geophys. Res. Lett*., **43**, doi:10.1002/2016GL067887.

Higgins, R. W., J.-K. E. Schemm, W. Shi, and A. Leetmaa, 2000: Extreme precipitation events in the western United States related to tropical forcing. *J. Clim*ate, **13**, 793-820.

Jones, C., F. Fujioka, and L. M. V. Carvalho, 2010: Forecast skill of synoptic conditions associated with Santa Ana winds in Southern California. *Mon. Wea. Rev.*, **138**, 4528–4541, doi: 10.1175/2010MWR3406.1.

Kalnay, E., M. Kanamitsu, R. Kistler, W. Collins, D. Deaven, L. Gandin, M. Iredell, S. Saha, G. White, J. Woollen, Y. Zhu, A. Leetmaa, R. Reynolds, M. Chelliah, W. Ebisuzaki, W. Higgins, J. Janowiak, K. Mo, C. Ropelewski, J. Wang, R. Jenne, and D. Joseph, 1996: The NCEP/NCAR 40-year reanalysis project. *Bull. Amer. Meteor. Soc.*, **77**, 437–471.

Keeley, J. E., C. J. Fotheringham, and M. A. Moritz, 2004: Lessons from the 2003 wildfires in southern California. *J. Forecast*., **102**, 26–31.

Keeley, J. E., H. Safford, C. J. Fotheringham, J. Franklin, and M. Moritz, 2009: The 2007 Southern California wildfires: Lessons in complexity. *J. Forecast*., **107**, 287–296.

Madden, R., and P. Julian, 1994: Observations of the 40–50 day tropical oscillation – a review. *Mon Wea. Rev*., **122**, 814–837.

Mass, C, and D. Owens, 2019: The northern California wildfires of 8-9 October 2017. *Bull. Amer. Meteor. Soc*., 23-5-256, doi:10.1175/BAMS-D-18-0037.1.

Mundhenk, B., E. Barnes, E. Maloney, and C. Baggett, 2018. Skillful empirical subseasonal prediction of landfalling atmospheric river activity using the Madden–Julian oscillation and quasi-biennial oscillation. *npj Clim. Atmos. Sci.*, 1:20177, doi:10.1038/s41612-017-0008-2.

Raphael, M. N., 2003: The Santa Ana winds of California. *Earth Interact*., **7**, 1–13, doi:10.1175/1087-3562(2003)007,0001:TSAWOC.2.0.CO;2.

Raphael, M., and J. Finley, 2007: The relationship between El Niño and the duration and frequency of the Santa Ana Winds of southern California. *The Professional Geographer*, **59**, 184-192, doi: 10.1111/j.1467-9272.2007.00606.x.

Rolinski, T., S. Capps, and W. Zhuang, 2019: Santa Ana winds: A descriptive climatology. *Wea. Forecasting*, **34**, 257-275, doi: 10.1175/WAF-D-18-0160.1.

Saha, S., and Coauthors, 2010: The NCEP climate forecast system reanalysis. . *Bull. Amer. Meteor. Soc.*, **91**: 1015–1057.

Sardeshmukh, P. D. and Hoskins, B. J., 1988: The generation of global rotational flow by steady idealized tropical divergence. *J. Atmos. Sci*., **45**, 1228–1251.

Swain, D., D. Singh, D. Horton, J. Mankin, T. Ballard, and N. Diffenbaugh, 2017: Remote linkages to anomalous winter atmospheric ridging over the northeastern Pacific. *J. Geophys. Res*., **12**, 194-209, doi: doi:10.1002/2017JD026575.

Westerling, A., D. R. Cayan, T. J. Brown, B. L. Hall, and L. G. Riddle, 2004: Climate, Santa Ana winds and autumn wildfires in southern California. *Eos, Trans. Amer. Geophys. Union*, **85**, 289–296, doi:10.1029/2004EO310001.

Wheeler, M. C., and H. H. Hendon, 2004: An all season realtime multivariate MJO index: Development of an index for monitoring and prediction. *Mon. Wea. Rev.*, **132**, 1917–1932.

Wolter, K., and M. S. Timlin, 2011: El Niño/Southern Oscillation behaviour since 1871 as diagnosed in an extended multivariate ENSO index (MEI.ext). *Intl. J. Climatology*, **31**, 1074-1087.